

Impact of BiBO₃, NaF and BiF₃ Substitution on the Thermoelectric Properties of Bi₂Ca₂Co₂O_y Ceramics

Iamze Kvartskhava¹, Nikoloz Margiani¹, Vakhtang Zhghamadze¹, Giorgi Mumladze¹, Giorgi Kakhniashvili¹, Natia Margiani¹, and Irina Khomeriki²

¹Georgian Technical University, Institute of Cybernetics, Z. Anjaparidze str., 1st Ln., N6, 0186, Tbilisi, Georgia, iakvartskhava@gmail.com, n.margiani@gtu.ge, vakhtang66@gmail.com, g.mumladze@gtu.ge, georgekakhniashvili13081955@gmail.com, natiamargiani@gmail.com

²Georgian Technical University, Faculty of Informatics and Control Systems, 77 Kostava str., 0160, Tbilisi, Georgia, i.khomeriki@gtu.ge

Abstract - In this work, we studied the impact of (i) partial substitution of bismuth oxide (Bi₂O₃) by bismuth borate (BiBO₃), (ii) dual-substitution of Bi₂O₃ by BiBO₃ and sodium fluoride (NaF), and (iii) dual-substitution of Bi₂O₃ by BiBO₃ and bismuth fluoride (BiF₃) on the thermoelectric characteristics of Bi₂Ca₂Co₂O_y layered cobaltite. Thermoelectric cobaltites were synthesized using the sol-gel method. The phase composition of prepared materials was examined by the X-ray diffraction (XRD) analysis. The values of power factor (PF) and figure of merit (ZT) were calculated through measurements of electrical resistivity (ρ), Seebeck coefficient (S), and thermal conductivity (k). The XRD analysis confirms that all the samples consist of a nearly pure Bi₂Ca₂Co₂O_y phase. When compared to the reference (pristine) sample, the dual NaF/BiBO₃ substitution leads to a sharp decrease in ρ due to the partial substitution of NaF for Bi₂O₃, which increases the concentration of charge carriers (holes). At the same time, partial substitution of BiF₃ for Bi₂O₃ led to a decrease in hole concentration and, hence, an increase in ρ . Seebeck coefficients were positive for all the samples, indicating p-type conductivity. The maximum PF and ZT values achieved in the NaF/BiBO₃ co-substituted composition are 18% and 13% higher, respectively, than the reference Bi₂Ca₂Co₂O_y.

Keywords: Thermoelectricity, Substitution, Sol-gel technique, Power factor, Figure of merit.

© Copyright 2025 Authors - This is an Open Access article published under the Creative Commons Attribution License terms (<http://creativecommons.org/licenses/by/3.0>). Unrestricted use, distribution, and reproduction in any medium are permitted, provided the original work is properly cited.

1. Introduction

Date Received: 2024-08-22
Date Revised: 2025-02-17
Date Accepted: 2025-03-02
Date Published: 2025-03-25

Due to the increasing global energy demand and climate change issues, the importance of environmentally friendly renewable energy technologies is growing. Many studies in this field focus on thermoelectric materials that can directly convert waste heat into electric power. The discovery of thermoelectric properties in complex cobalt oxides, NaCo₂O₄, Ca₃Co₄O₉ and Bi₂M₂Co₂O_y (M = Ca, Sr or Ba), opened the way to the systematic exploration and development of polycrystalline cobaltites for potential applications [1]-[4]. Metal oxides offer advantages over conventional non-oxide thermoelectric materials (intermetallic compounds and alloys) due to their environmental friendliness, ease of processing, high thermal and chemical stability, abundance, and low cost of raw materials. The thermoelectric conversion efficiency of materials is characterized by the dimensionless figure-of-merit $ZT = S^2T/\rho k$, where S represents the Seebeck coefficient, T is the absolute temperature, ρ denotes electrical resistivity, and k stands for total thermal conductivity [5]. The power factor $PF = S^2/\rho$ is an electrical component of the ZT formula that assesses output electrical power. However, a significant drawback of thermoelectric cobaltites is their low heat-to-electricity conversion efficiency compared to conventional materials [6]. Therefore, the challenge lies in improving electronic transport properties, such as electrical conductivity and the Seebeck coefficient, while also minimizing the phonon contribution to thermal transport by carefully selecting scattering centers [7]. Various strategies can improve

the efficiency of thermoelectric oxides, such as texturing, soft-chemistry techniques, and the incorporation of substituents and additives into these materials [8]-[12]. The sol-gel synthesis provides a promising method to enhance the conversion efficiency of thermoelectric materials by achieving exceptionally high chemical homogeneity. One of the main advantages of gel chemistry is its use of well-mixed solutions of molecular precursors, which ensures consistent homogeneity throughout the entire process, from the initial solution to the final product. Additionally, the high versatility of the sol-gel technique allows for easy modification of both the type and concentration of the substituents and additives [13]. The *p*-type $\text{Bi}_2\text{Sr}_2\text{Co}_2\text{O}_y$ and $\text{Bi}_2\text{Ca}_2\text{Co}_2\text{O}_y$ cobaltites are promising materials for thermoelectric applications [14]. Sol-gel-derived $\text{Bi}_2\text{Sr}_2\text{Co}_2\text{O}_y$ and $\text{Bi}_2\text{Ca}_2\text{Co}_2\text{O}_y$ showed better characteristics than those made by the conventional solid-state reaction technique [15]-[18]. We recently reported an improvement in the *ZT* of the bismuth borate (BiBO_3)-incorporated $\text{Bi}_2\text{Sr}_2\text{Co}_2\text{O}_y$, which was prepared by the sol-gel method [12]. It was shown that the *ZT* value of BiBO_3 -added $\text{Bi}_2\text{Sr}_2\text{Co}_2\text{O}_y$ increases by 39 % at 573 K compared to the reference specimen. In this work, we studied the impact of (i) partial substitution of bismuth oxide (Bi_2O_3) by BiBO_3 , (ii) dual-substitution of Bi_2O_3 by BiBO_3 and sodium fluoride (NaF), and (iii) dual-substitution of Bi_2O_3 by BiBO_3 and bismuth fluoride (BiF_3) on the thermoelectric characteristics of $\text{Bi}_2\text{Ca}_2\text{Co}_2\text{O}_y$ layered cobaltite.

2. Materials and Methods

The Reference, BiBO_3 -substituted as well as BiBO_3/NaF and $\text{BiBO}_3/\text{BiF}_3$ dual substituted samples with the nominal compositions: $\text{Bi}_2\text{Ca}_2\text{Co}_2\text{O}_y$ (reference), $\text{Bi}_{1.9925}\text{Ca}_2\text{Co}_2(\text{BiBO}_3)_{0.0075}\text{O}_y$, $\text{Bi}_{1.8925}\text{Ca}_2\text{Co}_2(\text{NaF})_{0.10}(\text{BiBO}_3)_{0.0075}\text{O}_y$, and $\text{Bi}_{1.8925}\text{Ca}_2\text{Co}_2(\text{BiF}_3)_{0.10}(\text{BiBO}_3)_{0.0075}\text{O}_y$ were prepared by the sol-gel method using appropriate amounts of $\text{Bi}(\text{NO}_3)_3 \cdot 5\text{H}_2\text{O}$ (≥ 98 %, Thermo Scientific), CaCO_3 (≥ 99 %, Sigma-Aldrich), $\text{Co}(\text{NO}_3)_2 \cdot 6\text{H}_2\text{O}$ (≥ 99 %, Thermo Scientific), BiBO_3 (≥ 99 %, RESEARCH-LAB), NaF (≥ 99.9 %, Sigma-Aldrich), and BiF_3 (99 %, Thermo Scientific) powders as starting materials with citric acid ($\text{C}_6\text{H}_8\text{O}_7$) and ethylene glycol ($\text{C}_2\text{H}_6\text{O}_2$) as chelating agents. Afterwards, the 4 batches were moved to a magnetic hot plate stirrer (SMHS-3, Nabitex Scientific GmbH). The stirring rate was set from 400 to 500 rpm, and the temperature was maintained at 363 K for approximately 50 minutes. The substance levels were carefully monitored until the mixture reached a gel-like

consistency with a sharp pink colour. The gels were then transferred to alumina crucibles and dried in an oven at a temperature range of 353 to 443 K for 4 h. Once the gel masses turned brown and stopped expanding in the crucibles, thermal processing continued by heating the materials to 773 K to burn off any excess organic compounds completely. The resulting materials were ground manually in an agate mortar to break the agglomerates, followed by calcination at temperatures ranging from 1033 to 1068 K for 25 hours in a furnace, with intermediate grinding. Finally, the calcined powders were pressed into pellets at 220 MPa and sintered at 1098 K for 17 h. The density of pellets was determined by Archimedes' method, taking 6.35 g/cm^3 as the theoretical value [19]. The phase composition of the prepared materials was analyzed using X-ray diffraction (XRD, Dron-3M diffractometer, $\text{Cu K}\alpha$ radiation). The temperature dependence of the resistivity $\rho(T)$ and Seebeck coefficient $S(T)$ was measured simultaneously from room temperature to 973 K with a laboratory-made setup equipped with a KEITHLEY DMM6500 multimeter. Electrical transport measurements were performed on bar-shaped samples with dimensions of $\sim 13 \times 7 \times 2.5 \text{ mm}^3$. Thermal conductivity was determined from 300 to 573 K using the "Hot Disk TPS 500 thermal constants analyzer". Finally, values of *PF* and *ZT* were calculated to assess the thermoelectric performance of the synthesized cobaltite materials.

3. Results and Discussion

Figure 1 displays the XRD patterns of the prepared compositions, which closely match previously reported results for the $\text{Bi}_2\text{Ca}_2\text{Co}_2\text{O}_y$ system [8]-[9]. Only trace amounts of secondary phases were detected.

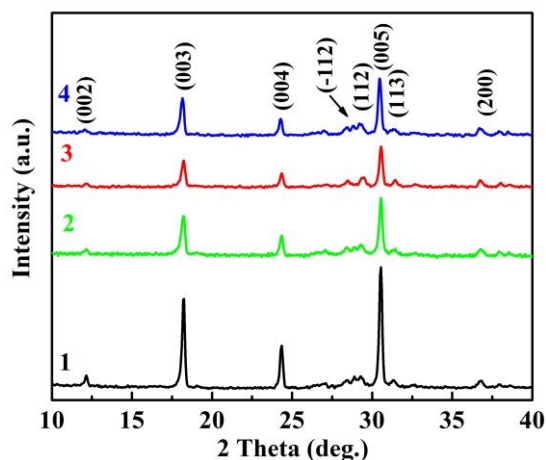


Figure 1. X-ray diffraction patterns. 1- $\text{Bi}_2\text{Ca}_2\text{Co}_2\text{O}_y$,
 2 - $\text{Bi}_{1.9925}\text{Ca}_2\text{Co}_2(\text{BiBO}_3)_{0.0075}\text{O}_y$,
 3 - $\text{Bi}_{1.8925}\text{Ca}_2\text{Co}_2(\text{NaF})_{0.10}(\text{BiBO}_3)_{0.0075}\text{O}_y$,
 4 - $\text{Bi}_{1.8925}\text{Ca}_2\text{Co}_2(\text{BiF}_3)_{0.10}(\text{BiBO}_3)_{0.0075}\text{O}_y$.

The densities of the prepared materials are similar and correspond to approximately 96-98 % of the theoretical value. Figure 2 illustrates the temperature dependence of the resistivity, Seebeck coefficient and power factor. Both the single BiBO_3 -substituted and double NaF/BiBO_3 -substituted materials exhibit a decrease in resistivity, which is advantageous for enhancing thermoelectric performance. The lowest resistivity value at 973 K, equal to $29.5 \text{ m}\Omega\cdot\text{cm}$, was found for the NaF/BiBO_3 double-substituted sample, which is 1.3-fold smaller than for reference $\text{Bi}_2\text{Sr}_2\text{Co}_2\text{O}$. This result is due to the partial substitution of NaF for Bi_2O_3 , which increases the concentration of charge carriers (holes). At the same time, partial substitution of BiF_3 for Bi_2O_3 led to a decrease in hole concentration and, hence, an increase in ρ . Seebeck coefficients were positive for all the samples, indicating p -type conductivity. The value of S for the NaF/BiBO_3 co-substituted composition at 973 K is 4–6 % lower than that of the reference, BiBO_3 -substituted, and $\text{BiF}_3/\text{BiBO}_3$ co-substituted samples. Positive values of the Seebeck coefficient, indicating p -type conductivity in all samples, increase as the temperature rises above 480 K (Figure 2b). Combining the values of the S and ρ , the PF was calculated and plotted in Figure 2c. The maximum PF value attained in the NaF/BiBO_3 double-substituted composition, $0.16 \text{ mW}/(\text{m}\cdot\text{K}^2)$, is 18% higher than the reference $\text{Bi}_2\text{Ca}_2\text{Co}_2\text{O}_y$. Consequently, the PF of the NaF/BiBO_3 double-substituted sample exceeds the values reported in the literature for both reference and doped $\text{Bi}_2\text{Ca}_2\text{Co}_2\text{O}_y$ compositions. These compositions were prepared via various methods, including the sol-gel process [11],[17], conventional solid-state sintering [17],[20] and a combination of high-energy ball milling followed by hot pressing sintering [9].

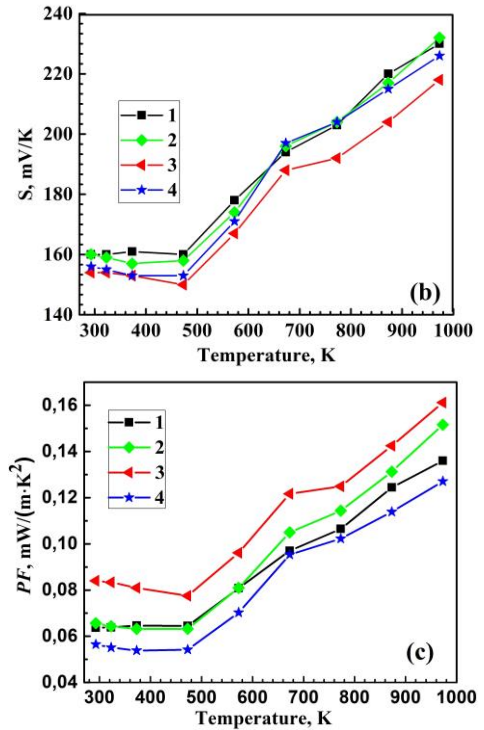
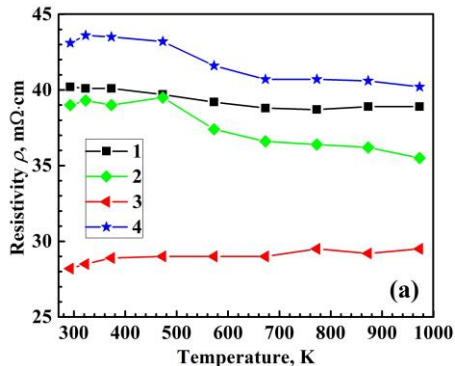


Figure 2. Temperature dependence of (a)-resistivity, (b)-Seebeck coefficient, and (c)-power factor. 1- $\text{Bi}_2\text{Ca}_2\text{Co}_2\text{O}_y$,
 2 - $\text{Bi}_{1.9925}\text{Ca}_2\text{Co}_2(\text{BiBO}_3)_{0.0075}\text{O}_y$,
 3 - $\text{Bi}_{1.8925}\text{Ca}_2\text{Co}_2(\text{NaF})_{0.10}(\text{BiBO}_3)_{0.0075}\text{O}_y$,
 4 - $\text{Bi}_{1.8925}\text{Ca}_2\text{Co}_2(\text{BiF}_3)_{0.10}(\text{BiBO}_3)_{0.0075}\text{O}_y$.

Figure 3 displays the measured total thermal conductivity, lattice (phonon) k_{latt} and electronic k_{el} components of total thermal conductivity, and the calculated figure of merit for the prepared materials from 293 to 573 K. The electronic thermal conductivity, k_{el} was determined through the Wiedemann–Franz law as $k_{el} = LT/\rho$, where $L=2.44 \times 10^{-8} \text{ V}^2\cdot\text{K}^{-2}$ is the Lorenz number, T is the absolute temperature, and ρ is the electrical resistivity [9]. Then, the phonon thermal conductivity was separated from the total thermal conductivity as $k_{ph} = k - k_{el}$. Double BiBO_3/NaF substitution increases the k value of the $\text{Bi}_2\text{Ca}_2\text{Co}_2\text{O}_y$ system while the single BiBO_3 and double $\text{BiBO}_3/\text{BiF}_3$ substituents cause the decrease of k . In all samples, k_{el} is significantly lower than total thermal conductivity, with k_{ph} dominating in the k . Double BiBO_3/NaF substituted sample possesses a higher ZT value than the reference sample due to an increased electrical conductivity. The ZT for double BiBO_3/NaF substituted samples reaches 0.036 at 573 K, which is 13 % higher than that of the reference $\text{Bi}_2\text{Ca}_2\text{Co}_2\text{O}_y$. This value of ZT is higher than previously reported in [18] for the solid-state and sol-gel

processed $\text{Bi}_2\text{Ca}_2\text{Co}_{1.7}\text{O}_y$ and lies between sol-gel and polymer solution methods.

3 – $\text{Bi}_{1.8925}\text{Ca}_2\text{Co}_2(\text{NaF})_{0.10}(\text{BiBO}_3)_{0.0075}\text{O}_y$,
 4 – $\text{Bi}_{1.8925}\text{Ca}_2\text{Co}_2(\text{BiF}_3)_{0.10}(\text{BiBO}_3)_{0.0075}\text{O}_y$.

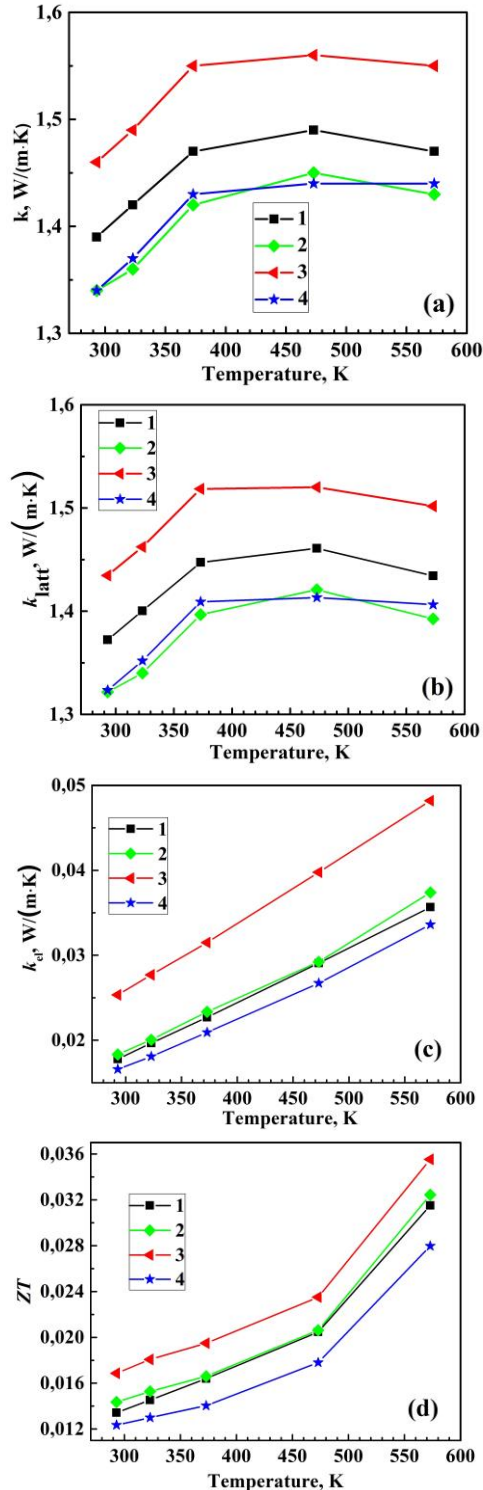


Figure 3. Temperature dependence of (a)-total thermal conductivity, (b)-lattice component, (c)-electronic component and (d)-figure of merit. 1– $\text{Bi}_2\text{Ca}_2\text{Co}_2\text{O}_y$, 2 – $\text{Bi}_{1.9925}\text{Ca}_2\text{Co}_2(\text{BiBO}_3)_{0.0075}\text{O}_y$,

4. Conclusion

We investigated the sol-gel derived $\text{Bi}_2\text{Sr}_2\text{Co}_2\text{O}_y$ samples that were either partially substituted with BiBO_3 or partially co-substituted with BiBO_3/NaF and $\text{BiBO}_3/\text{BiF}_3$. The maximum PF and ZT values of the NaF/BiBO_3 co-substituted composition were 18 % and 13 % higher, respectively, compared to the reference $\text{Bi}_2\text{Ca}_2\text{Co}_2\text{O}_y$. Identifying the optimal amounts of substituents could further enhance the thermoelectric performance of $\text{Bi}_2\text{Ca}_2\text{Co}_2\text{O}_y$ cobaltite.

Acknowledgements

This work was supported by the International Science and Technology Center (ISTC) [Project # GE-2776/Enhancing the thermoelectric conversion performance of cobalt-based oxide materials through doping and microstructure modulation].

References

- [1] I. Terasaki, Y. Sasago, K. Uchinokura. Large thermoelectric power in NaCo_2O_4 single crystals. *Physical Review B*. 1997, 56, R12685–R12687. DOI: <https://doi.org/10.1103/PhysRevB.56.R12685>
- [2] R. Funahashi, I. Matsubara, H. Ikuta, T. Takeuchi, U. Mizutani, S. Sodeoka. An oxide single crystal with high thermoelectric performance in air. *Japanese Journal of Applied Physics*. 2000, 39, L1127–L1129. <https://dx.doi.org/10.1143/JJAP.39.L1127>
- [3] C. Masset, C. Michel, A. Maignan, M. Hervieu, O. Toulemonde, F. Studer, B. Raveau, J. Hejtmanek. Misfit-layered cobaltite with an anisotropic giant magnetoresistance: $\text{Ca}_3\text{Co}_4\text{O}_9$. *Physical Review B*. 2000, 62, 166–175. DOI:<https://doi.org/10.1103/PhysRevB.62.166>
- [4] R. Funahashi, I. Matsubara, S. Sodeoka. Thermoelectric properties of $\text{Bi}_2\text{Sr}_2\text{Co}_2\text{O}_x$ polycrystalline materials. *Applied Physics Letters*. 2000, 76, 2385–2387. <https://doi.org/10.1063/1.126354>
- [5] He, J.; Liu, Y.; Funahashi, R. Oxide thermoelectrics: The challenges, progress, and outlook. *Journal of Materials Research*. 2011, 26, 1762–1772. <https://doi.org/10.1557/jmr.2011.108>
- [6] K. Fujimoto, M. Gibu, Y. Yamaguchi, A. Aimi, K. Nishio, O. Rabin, I. Takeuchi. Thermoelectric properties of bismuth-substituted calcium manganite $\text{Ca}_{1-x}\text{Bi}_x\text{MnO}_{3-\delta}$ prepared via the electrostatic spray deposition method. *Journal of the Ceramic Society of*

- Japan.* 2017, 125, 308-312.
DOI: <https://doi.org/10.2109/jcersj2.16277>
- [7] M. Ohtaki, Recent aspects of oxide thermoelectric materials for power generation from mid-to-high temperature heat source. *Journal of the Ceramic Society of Japan.* 2011, 119, 770-775. <https://doi.org/10.2109/jcersj2.119.770>
- [8] Can Özçelik, Tolga Depci, Mehmet Gürsul, Gizem Çetin, Bekir Özçelik, Miguel A. Torres, Maria A. Madre, Andres Sotelo. Drastic microstructural modification of $\text{Bi}_2\text{Ca}_2\text{Co}_2\text{O}_y$ ceramics by Na doping and laser texturing. 2022, *Boletín de la Sociedad Espanola de Cerámica y Vidrio.* 61, 634-640, <https://doi.org/10.1016/j.bsecv.2021.06.003>
- [9] Song-Tao Dong, Miao-Cheng Yu, Zhuang Fu, Yang-Yang Lv, Shu-Hua Yao, Y.B. Chen, High thermoelectric performance of NaF-doped $\text{Bi}_2\text{Ca}_2\text{Co}_2\text{O}_y$ ceramic samples, 2022, *Journal of Materials Research and Technology*, 17, 1598-1604, <https://doi.org/10.1016/j.jmrt.2022.01.102>
- [10] M.A. Madre, Sh. Rasekh, K. Touati, C. Salvador, M. Depriester, M.A. Torres, P. Bosque, J.C. Diez, A. Sotelo, From nanosized precursors to high performance ceramics: The case of $\text{Bi}_2\text{Ca}_2\text{Co}_{1.7}\text{O}_x$, *Materials Letters.* 2017, 191, 14-16, <https://doi.org/10.1016/j.matlet.2017.01.03>
- [11] Amaveda, H., Madre, M.A., Mora, M., Torres M. A., Sotelo A. Anomalous grain growth in sintered $\text{Bi}_2\text{Ca}_2\text{Co}_{2-x}\text{Cu}_x\text{O}_y + \text{Ag}$ ceramic composites by Cu doping. *Journal of Materials Science: Materials in Electronics.* 34, 9, 2023. <https://doi.org/10.1007/s10854-022-09416-x>
- [12] Margiani, N.; Zhghamadze, V.; Mumladze, G.; Takeda, M.; Kvartskhava, I. Thermoelectric properties of BiBO_3 -added $\text{Bi}_2\text{Sr}_2\text{Co}_2\text{O}_y$ ceramics. *Journal of the Ceramic Society of Japan.* 2025, in press.
- [13] J. M. Nedelec, L. Courtheoux, E. Jallot, C. Kinowski, J. Lao, P. Laquerriere, C. Mansuy, G. Renaudin, S. Turrell. Materials Doping Through Sol-Gel Chemistry: A Little Something Can Make a Big Difference. *Journal of Sol-Gel Science and Technology.* 2008 46, 259–271. <https://doi.org/10.1007/s10971-007-1665-0>.
- [14] S. Rasekh, G. Constantinescu, M. A. Madre, M. Torres, J. Diez, A. Sotelo. Processing effects on the thermoelectric properties of $\text{Bi}_2\text{Ca}_2\text{Co}_{1.7}\text{O}_x$ ceramics. 2014, *Boletín de la Sociedad Espanola de Cerámica y Vidrio.* 53, 207-212. <https://api.semanticscholar.org/CorpusID:204009217>
- [15] Rubešová, K.; Hlásek, T.; Jakeš, V.; Huber, Š.; Hejtmánek, J.; Sedmidubský, D. Effect of a powder compaction process on the thermoelectric properties of $\text{Bi}_2\text{Sr}_2\text{Co}_{1.8}\text{O}_x$ ceramics. *Journal of the European Ceramic Society.* 2015, 35, 525-531. DOI:10.1016/j.jeurceramsoc.2014.08.037
- [16] K. Rubešová, T. Hlásek, V. Jakeš, Š. Huber, J. Hejtmánek, D. Sedmidubský, Water based sol-gel methods used for Bi-222 thermoelectrics preparation. *Journal of Sol-Gel Science and Technology.* 64, 93-99, 2012. DOI 10.1007/s10971-012-2831-6
- [17] Torres, M.A.; Sotelo, A.; Rasekh, Sh.; Serrano, I.; Constantinescu, G.; Madre, M.A.; Diez, J.C. Mejora de Las Propiedades Termoeléctricas de $\text{Bi}_2\text{Sr}_2\text{Co}_{1.8}\text{O}_x$ Por Métodos de Síntesis En Disolución. *Boletín de la Sociedad Espanola de Cerámica y Vidrio.* 2012, 51, 1–6.
- [18] A. Sotelo, Sh. Rasekh, M.A. Madre, E. Guilmeau, S. Marinel, J.C. Diez. Solution-based synthesis routes to thermoelectric $\text{Bi}_2\text{Ca}_2\text{Co}_{1.7}\text{O}_x$, *Journal of the European Ceramic Society.* 2011, 31, 1763-1769. <https://doi.org/10.1016/j.jeurceramsoc.2011.03.008>
- [19] Muguerra H, Rivas-Murias B, Traianidis M, Henrist C, Vertruyen B, Cloots R. Improvement of the thermoelectric properties of $[\text{Bi}_{1.68}\text{Ca}_2\text{O}_{4-\delta}]^{\text{RS}}[\text{CoO}_2]_{1.69}$ cobaltite by chimie douce methods. *Journal of solid state chemistry.* 2010, 183:1252–7. <https://doi.org/10.1016/j.jssc.2010.03.030>
- [20] Hao, H. S., He, Q. L., & Zhao, L. M. 2011, Thermoelectric Properties of Cu-Substituted $\text{Bi}_2\text{Ca}_2\text{Co}_2\text{O}_y$ Misfit Oxides. *Advanced Materials Research,* 284–286, 2263–2267. <https://doi.org/10.4028/www.scientific.net/amr.284-286.2263>